Environmental Science & Technology

Critical Review

Cite This: Environ. Sci. Technol. 2018, 52, 2468−2481

pubs.acs.org/est

Environmentally Persistent Free Radicals: Insights on a New Class of Pollutants

Eric P. Vejerano,*[,†] Guiying Rao,[†] Lavrent Khachatryan,[‡] Stephania A. Cormier,[§,∥] and Slawo Lomnicki[⊥]

[†]Center for Environmental Nanoscience and Risk, Department of Environmental Health Sciences, Arnold School of Public Health, University of South Carolina, Columbia South Carolina 29208, United States

[‡]Department of Chemistry, Louisiana State University, Baton Rouge, Louisiana 70803, United States;

[§]Department of Biological Sciences, Louisiana State University, Baton Rouge, Louisiana 70803, United States

[∥]Comparative Biomedical Sciences, Louisiana State University School of Veterinary Medicine, Baton Rouge, Louisiana 70803, United States

[⊥]Department of Environmental Sciences, Louisiana State University, Baton Rouge, Louisiana 70803, United States

ABSTRACT: Environmentally persistent free radicals, EPFRs, exist in significant concentration in atmospheric particulate matter (PM). EPFRs are primarily emitted from combustion and thermal processing of organic materials, in which the organic combustion byproducts interact with transition metal-containing particles to form a free radical-particle pollutant. While the existence of persistent free radicals in combustion has been known for over half-a-century, only recently that their presence in environmental matrices and health effects have started significant research, but still in its infancy. Most of the experimental studies conducted to understand the origin and nature of EPFRs have focused primarily on nanoparticles that are supported on a larger micrometer-sized particle that mimics incidental nanoparticles formed during combustion. Less is known on the extent by which EPFRs may form on engineered nanomaterials (ENMs) during combustion or thermal treatment. In this critical and timely review, we summarize important findings on EPFRs and discuss their potential to form on pristine ENMs as a new research direction. ENMs may form EPFRs that may differ in type and concentration compared to nanoparticles that are supported on larger particles. The lack of basic data and fundamental knowledge about the interaction of combustion byproducts with ENMs under high-temperature and oxidative conditions present an unknown environmental and health burden. Studying the extent of ENMs on catalyzing EPFRs is important to address the hazards of atmospheric PM fully from these emerging environmental contaminants.

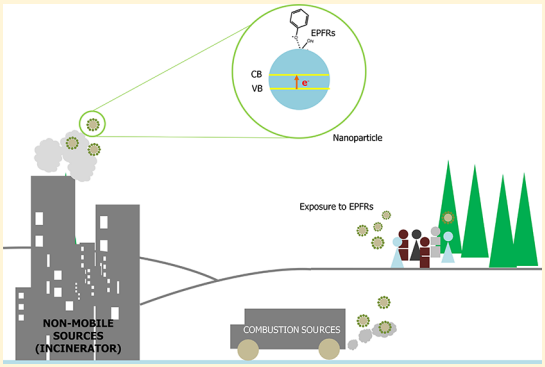

INTRODUCTION

The interaction of ENMs and organic materials during thermal treatment in forming and stabilizing long-lived EPFRs remains unaddressed. ENMs are manufactured particles with dimension ranging from 1 to 100 nm at least in one dimension. Unlike previously identified atmospheric gas-phase free radicals that exist for only a fraction of a second, EPFRs that are bound to particles have lifetimes of minutes and up to several months.[1,2] Such extreme lifetimes of EPFRs allow them to be transported over long distances intact. This potential for long-range transport present a higher risk to EPFR exposure. The inhalation of EPFRs have been associated with a variety of diseases.[3−6] Note however that exposure to EPFRs depends on the lifetimes of airborne particles; atmospheric ultrafine particles can rapidly coagulate to the accumulation mode (100 nm to 2.5 μm)—the atmospheric lifetimes of which is only up to 2 weeks because wet deposition is a major sink for these particles.[7]

The influx of products containing ENMs on the consumer market continues to rise, and by 2020, nanotechnology is expected to contribute an estimated US$3 trillion to the global economy.[8] The behavior of ENMs subjected under high-temperature and oxidative treatment such as during incineration of nanowaste or during accidental fires on their potential to form EPFRs remains uncertain. In the coming years, incinerators will burn ∼8600 tons/year of ENMs globally.[9] Although researchers predict that <3% of incinerated ENMs will enter the atmosphere,[9] there are reasons to be concerned not only about the inhalation of ENMs but also from exposure to combustion byproducts (e.g., EPFRs) catalyzed by ENMs.

Received: August 29, 2017
Revised: February 7, 2018
Accepted: February 14, 2018
Published: February 14, 2018

DOI: 10.1021/acs.est.7b04439
Environ. Sci. Technol. 2018, 52, 2468−2481

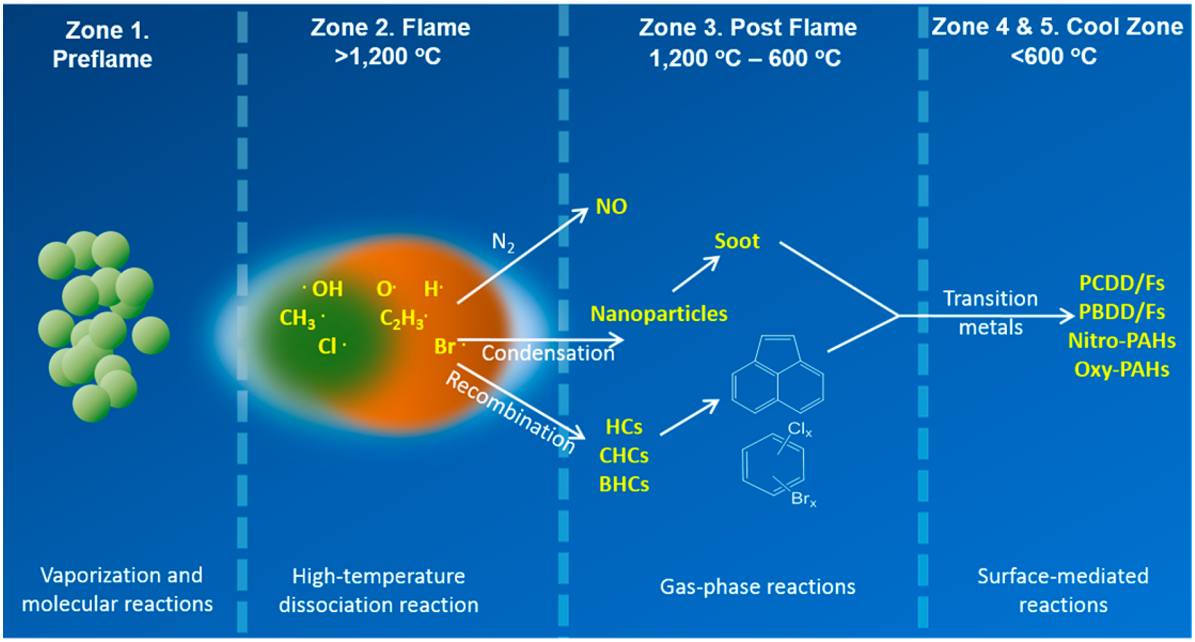

Figure 1. Zone theory of combustion. Recombination of atoms or small molecules in the flame zone forms hydrocarbons (HCs), chlorinated hydrocarbons (CHCs), and brominated hydrocarbons (BHCs) in the post flame zone as the temperature decreases. Surface-mediated reactions catalyzed by transition metals at temperature lower than 600 °C form polychlorinated dibenzofurans (PCDFs), polychlorinated dibenzo-*p*-dioxins (PCDDs), and polycyclic aromatic hydrocarbons (nitro-PAHs and oxy-PAHs). Adapted from Cormier et al., 2006.

Additionally, the potential for exposure via inhalation of particles (the most studied) exceeds dermal or oral routes.[10]

The few studies that have investigated ENMs in solid waste and polymer matrices subjected to thermal treatment only explored ENMs' effect on the emission of combustion byproducts;[11−13] the release of ENMs from matrices;[14,15] and the partitioning of ENMs.[16] To our knowledge, there is a lack of studies investigating the impact of materials that already exist as nanoparticles before being incinerated on forming and stabilizing EPFRs.

Furthermore, previous studies on the effect of nanoparticles' properties (e.g., size, composition, etc.) on EPFRs have mimic only the formation of EPFRs on incidental nanoparticles that are formed during combustion, but not on pristine ENMs.[1,17,18] These incidental nanoparticles formed as "islands" or nanoclusters that are supported on large micrometer-size particles. The formation of EPFRs is not exclusive to combustion reaction; a similar process occurs in soils that contain a high concentration of metals and organic materials under ambient soil condition such as those in some Superfund sites.[19−22]

In this critical review, we present the important findings generated from over a decade of research on EPFRs as a recently discovered class of environmental pollutants with significant health effects. We also discuss the concepts and principles in surface science that may underpin the basis as to the potential of ENMs to form EPFRs. We discuss the changes to the properties of ENMs when subjected to incineration/thermal treatment and the impact of such shifts on the formation of EPFRs. While the focus of this review is the formation of EPFRs on surfaces, EPFRs can also form via gas-phase reactions.[23] Additionally, a possible source of EPFRs in atmospheric particles may include contribution from secondary organic aerosol (SOA). We discuss this topic briefly, but EPFRs on SOA merits its own review.

Nature, Origin, and Emission of EPFRs. A free radical is an atom or molecule that contains at least one unpaired electron; because of this unpaired electron, a free radical is highly reactive. Free radicals have lifetimes typically a fraction of a second or much less (for instance, an OH radical has a lifetime of ~10^{-9} s). However, EPFRs from combustion-generated PM exist for much longer times.[1,2,18,24] EPFRs are highly stable—meaning they do not easily decompose after being formed, and are highly persistent—meaning they exhibit extremely long lifetimes (ranging from the order of minutes to months). Lyons, Ingrams, and their colleagues, first reported the presence of persistent free radicals in coals, chars, and soot in the 1950s.[25,26] It was only after three decades when Pryor and colleagues linked the health impacts of persistent free radicals present in cigarette smoke by demonstrating that these pollutants undergo catalytic cycling.[27−29] However, Dellinger and colleagues were the first to describe the existence of persistent free radicals in environmental matrices including their presence in soil and airborne PM.[19,20,29,30]

EPFRs exist in different environmental matrices, including airborne PM,[30] fly ash,[31] and soils.[19] Only in the past decade that extensive research has begun to understand the properties, significance, and environmental and health relevance of EPFRs.

Dellinger and colleagues observed that EPFRs are present in fine and ultrafine atmospheric PM and induce DNA damage.[29] Measurement of PM in six U.S. cities revealed significant quantities of free radicals in PM with properties similar to that of semiquinone radicals, which had been confirmed by lab-generated EPFRs from burning fuels.[29] Aqueous extracts of these PM damage human lung epithelial cells and myeloid leukemia cells[29]—a response identical to those exerted by an incinerators' bottom ash.[32] Since this finding, a surface-associated semiquinone-type radical is believed to be responsible for such damage.[32]

Formation of EPFRs in Combustion System. The current conceptual model indicates that EPFRs are formed when combustion byproducts interact with transition metal oxide on PM. Electron paramagnetic resonance (EPR)

DOI: 10.1021/acs.est.7b04439
Environ. Sci. Technol. 2018, 52, 2468−2481

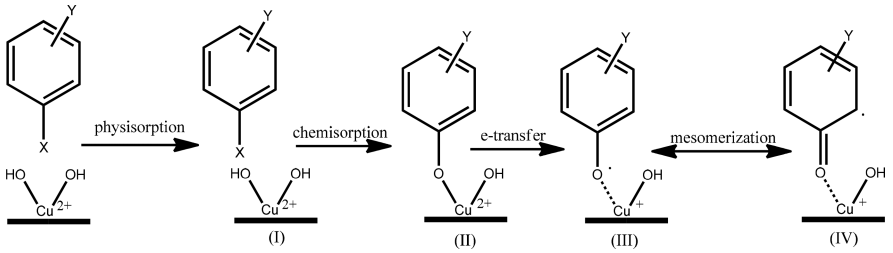

Figure 2. Conceptual mechanism of EPFR formation on a Cu(II)O surface.

measurement of free radicals on airborne PM revealed electronic *g*-factors that are consistent with an organic species.[31] The *g*-factor is the ratio of an electron's magnetic moment to its angular momentum. An unpaired electron in a different chemical environment exhibits a unique *g*-factor. Hence, the *g*-factor indicates the nature of the paramagnetic species. Because transition metals are known to catalyze surface-reactions and organic species interact with the surface of nanoparticles, transition metals are a key component in forming EPFRs.[1,2]

During incineration, combustion byproducts emitted from organic materials are subjected to different temperature and pressure. The zone theory of combustion divides the process into five distinct zones—each zone varies in the type and extent of combustion byproducts formed.[33] Of relevance to the formation of EPFRs is the surface-catalysis cool zone (zone 5) illustrated in Figure 1. The temperature at this zone ranges between 200 and <600 °C. In this zone, the reaction times between gas-phase species and the particle's surface for particles that are entrained in the flue gas are in the order of a few seconds and for particles deposited on the walls of the reactor, reaction times are up to several hours.[33] This low-temperature region favors the formation of resonance-stabilized aromatic EPFRs on the surfaces of particles.

Key Steps in EPFR Formation. We synthesized EPFRs in the lab first on Cu(II)O with chlorinated and hydroxylated benzenes and their derivatives.[1] We chose Cu because it is among the most abundant transition metals in PM.[34] The prevailing conceptual model on EPFR formation suggests that EPFRs are formed through a series of three important steps:[1,17] physisorption, chemisorption, and electron transfer.

Figure 2 illustrates the steps in the formation of EPFRs over a Cu(II)O surface. The first step involves the physical sorption of an aromatic molecule in which the hydroxyl and/or chlorine substituents interact with the surface of the transition metal oxide surface (Figure 2-I). The second step involves the chemisorption of the aromatic molecule on the surface via elimination of hydrogen chloride, water or both, depending on the type and number of substituents (Figure 2-II). Fourier-transform infrared study validated the second step as the OH stretching frequency at 3600 cm^{-1} disappears when the substituted benzene chemically binds on the surface.[35] The third step involves the transfer of an electron from the electron-rich oxygen atom to the surface of the metal, forming an EPFR (Figure 2-III). X-ray absorption near edge structures study revealed that Cu(II) is reduced to Cu(I) as supported by the shift to a lower binding energy when the molecular precursor adsorbs and reacts with the surface of the metal oxide.[36] The mechanism in Figure 2 implies that the formation of EPFRs requires hydroxylated metal oxides. Therefore, the potential for EPFR to form should correlate with the degree of hydroxylation as has been observed on α-Al(III)$_2$O$_3$ in forming phenoxy/phenolate species.[37]

Computational study on the formation of EPFRs from 2-chlorophenol on a $Cu_2O(110)$:CuO surface suggests that the dissociation of the hydrogen atom on the hydroxyl group from the oxygen atom can form either a chlorophenoxyl radical or a chlorophenoxyl moiety.[38] Cu(100) and $Cu_2O(110)$:CuO form 2-chlorophenoxy moiety to a similar extent as indicated by the similar energies.[38] Also, the orientation of the molecular precursor determines the extent of EPFR formation: a phenol molecule that is oriented almost perpendicular to an α-Al_2O_3 surface is more likely to physisorb[37] and form an EPFR.

Since that time, the prevailing conceptual mechanism of electron transfer involves a one-electron reduction, where the electron from the oxygen atom transfers to the metal surface, which reduces the metal. The surface-associated EPFR mesomerizes between its keto (Figure 2-III) and enol (Figure 2-IV) structures, forming a resonance-stabilized oxygen- or carbon-centered radical on the surface with an intact phenyl ring.[35,39] While the electron transfer step successfully explains EPFR formation for most of the metals we studied, Zn(II)O behaves differently as discussed later, and presumably other transition metal oxides as well.

Aside from Cu(II)O, EPFRs form and stabilize on other transition metal oxides such as on Ni(II)O, Fe(III)$_2$O$_3$, Ti(IV)O_2, and Zn(II)O.[1,2,18,24] The yields and lifetimes of EPFRs from substituted benzenes formed over different transition metal oxides vary as depicted in Figure 3. The concentration of EPFRs in a lab-synthesized PM is about 1−2 orders of magnitude higher than those in ambient PM because some of the EPFRs have decayed already.

Decay and Persistence of EPFRs. To date, the EPFRs we studied consist of an aromatic structure confined on a surface. Hence, these EPFRs are less susceptible to react with other molecules. The primary sink for the EPFRs in the atmosphere is their reaction with molecular oxygen, which converts EPFRs to molecular species. Oxygen can diffuse on the surface and can react with EPFRs. EPFRs decay as a pseudo-first order reaction since the concentration of oxygen is much higher than those of EPFRs.

The observed relaxation time (equivalently referred to as the 1/*e*-half-life, 1/*e*-fold time, or natural lifetime), a measure of the EPFRs' persistence, suggests that it depends both on the properties of the organic molecules and metal oxide surface. We define relaxation time as the time required for ∼37% of the initial concentration to decrease when exposed to air at ambient temperature and pressure.

The lifetimes of EPFRs measured from various substituted benzenes ranged from approximately half an hour to over several months. Figure 3A depicts the concentration of EPFRs bound on different metal oxides as well as the lifetime of EPFRs. The concentration of EPFRs formed over Ti(IV)O_2,

DOI: 10.1021/acs.est.7b04439
Environ. Sci. Technol. 2018, 52, 2468−2481

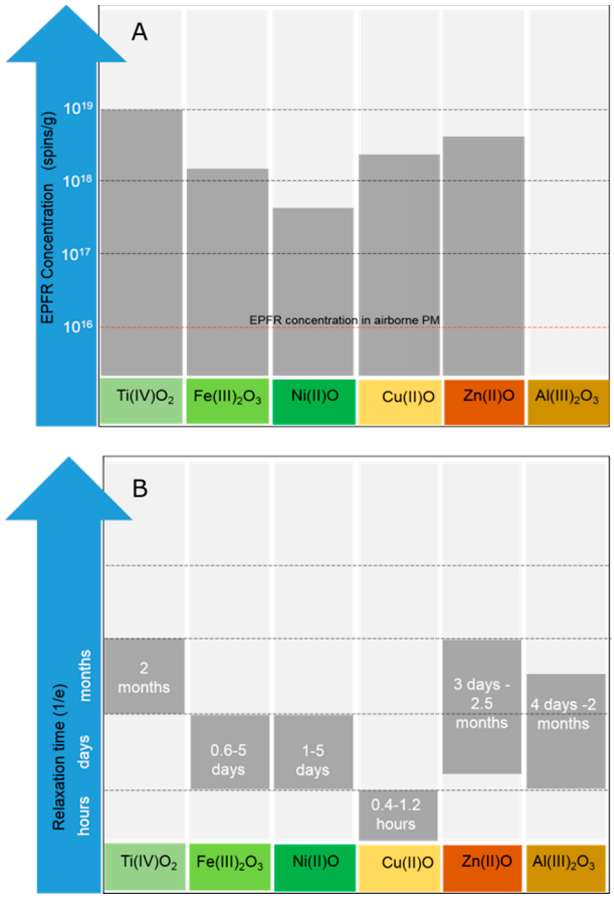

Figure 3. (A) Concentration of EPFRs formed on various transition metal oxide surfaces. EPFR concentration in airborne PM is in the order of 10^{16} spins/g (1 spin equals 1 free radical). EPFR concentration for $Al(III)_2O_3$ is unavailable. (B) Relaxation times of EPFRs formed on different metal oxide surfaces range from ~0.4 h to 2.5 months. We define relaxation time as the time required for ~37% of the EPFR concentration to decrease. Values used in the graphs were obtained from refs 1, 2, 17, 18, and 24.

$Fe(III)_2O_3$, Cu(II)O, and Zn(II)O are almost on a similar order (10^{18}–10^{19} spins/g) except those formed over Ni(II)O surface, which is the lowest (10^{17} spins/g).[1,2,18,24] EPFRs formed over a Zn(II)O[2] and $Ti(IV)O_2$[24] surfaces persist far longer than those that formed from similar precursors over $Fe(III)_2O_3$,[17] Ni(II)O,[18] and Cu(II)O[1] surfaces (Figure 3B). The relaxation times of EPFRs measured over Cu(II)O are on the order of hours while for both $Fe(III)_2O_3$ and Ni(II)O are on the order of days. Relaxation times for EPFRs over a Zn(II)O and $Ti(II)O_2$ surfaces are on the order of months. Such long relaxation times of EPFRs on Zn(II)O and $Ti(IV)O_2$ suggest an almost a year-long presence in ambient atmospheric PM. EPFRs on atmospheric $PM_{2.5}$ exhibit three modes of decay: fast, slow, and no measurable decay.[30] The latter two decay modes attest to the extreme persistence of EPFRs. We attribute the fast decay in both the real samples and the lab-synthesized samples to the decomposition of phenoxyl radicals to cyclopentadienyl radicals.[17] The presence of an intact highly resonance-stabilized phenyl ring accounts for their persistence,[35,39] and the property of the surface itself as discussed later. The EPFRs studied so far contain aromatic structures, which enable them to resist oxidation because of the presence of a localized electronic system that prevents the addition of oxygen molecules.

Based on the EPR studies and insights gained from mass spectrometry, the type of EPFRs constrained on surfaces of different transition metals include the following: phenoxyl, chlorophenoxyl, *o*-semiquinone, and *p*-semiquinone radicals (Figure 4).[1] In general, phenoxyl-type radicals persist longer compared to an *o*-semiquinone both of which persist longer than a *p*-semiquinone. Some of these EPFRs can decompose to the less persistent cyclopentadienyl radical.[17,40]

Molecular Byproducts from the Extraction of EPFRs. Conventional toxicity studies use solvents to extract the components in PM, which destroy EPFRs (i.e., a free radical is converted to a molecular species) and modify the toxicity of PM. For instance, Lichtveld and colleagues[41] demonstrated that PM in which the components have been phase separated or undergone post-treatment exhibit significantly different toxicity from PM that has been deposited directly into the air–liquid interface of cultured human lung cells. One may argue that in real inhalation scenario, PM will ultimately be dispersed in a respiratory fluid. But such fluid substantially differs in chemical properties from those of small a/protic solvents used for extracting components in PM for toxicity studies. Although, water, a protic solvent, is the dominant component of respiratory fluid, measurement of the persistence of EPFRs in different fractions of respiratory fluid indicates that they remain intact for a long time (relaxation time ~3 h) in serum and broncho-alveolar lavage fluid.[42] Such relaxation time is long enough to result in toxicities that were observed in animal studies. This result suggests that other components of respiratory fluid (e.g., proteins, surfactants, etc.) may protect EPFRs from decaying rapidly in liquid media. Hence, assessing

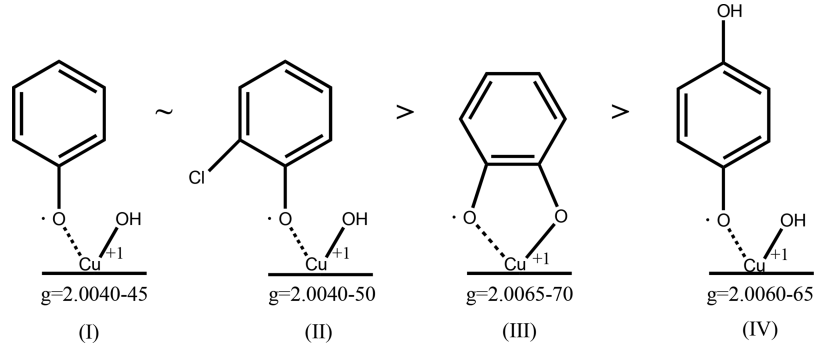

Figure 4. Type of free radicals responsible for the long lifetimes in PM. Phenoxyl radicals (I and II) are more persistent than *o*- and *p*-semiquinone radicals (III and IV). Adapted from Lomnicki et al., 2008 with permission from the American Chemical Society. Copyright 2008.

DOI: 10.1021/acs.est.7b04439
Environ. Sci. Technol. 2018, 52, 2468–2481

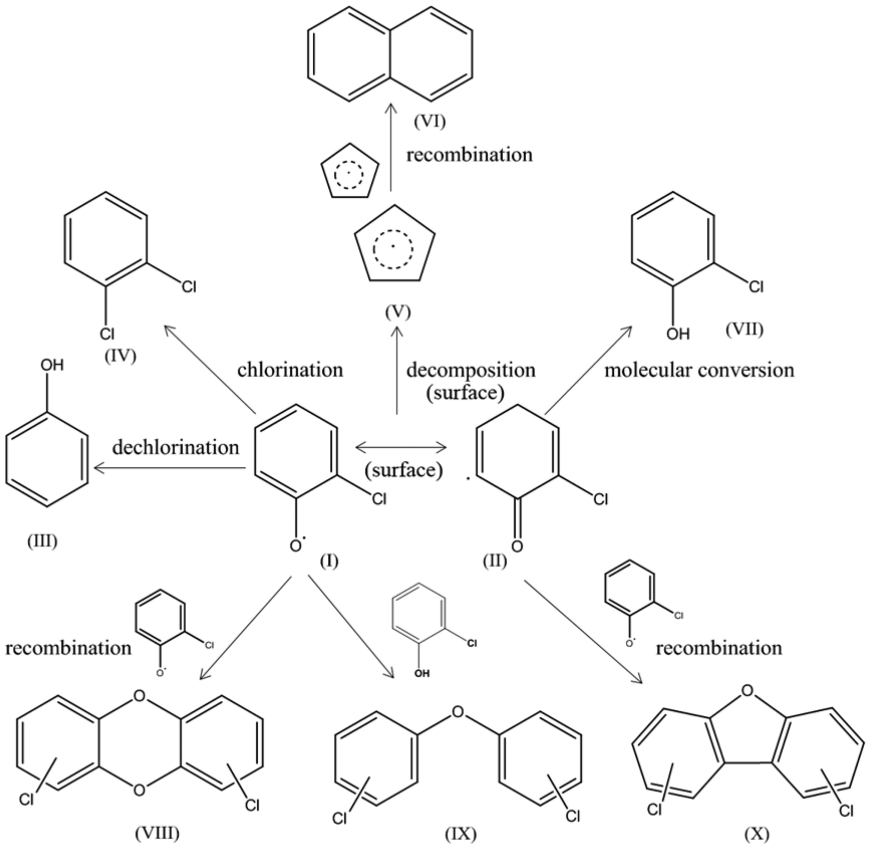

Figure 5. EPFRs are converted to molecular species by several reaction pathways, including, chlorination, hydrogen abstraction that converts them to their initial structure, and recombination reactions that produce dibenzofurans, dibenzo-*p*-dioxins, and biphenyl ethers, or biphenyls. For clarity, we omitted surface representation for structures I, II, and V. These free radicals are formed on surfaces as labeled. Organic structures that are formed on surfaces are labeled with "surfaces", otherwise, the species are formed in solutions. Adapted from Truong et al., 2010 with permission from the American Chemical Society. Copyright 2010.

EPFRs toxicity requires inhalation or deposition of the PM (e.g., intranasal deposition, instillation to the target organ, etc.). Conventional toxicity studies include only the effect from the molecular byproducts and exclude the contribution of EPFRs.

The efficiency of extracting EPFRs from PM depends on the properties of the solvents. Polar solvents with high dielectric constant and slightly acidic hydrogen (e.g., alcohols) efficiently extract EPFRs; while nonpolar solvents without donatable hydrogens (e.g., toluene) extract them poorly.[43]

Reactions of free radicals that are associated with surfaces have higher activation energies. However, when in solution, activation energies are lowered allowing for the reactions depicted in Figure 5 to occur. Extraction of EPFRs (oxygen- (Figure 5-I) and carbon-centered (Figure 5-II) radicals) with different solvents undergo a variety of reactions, which convert EPFRs to molecular byproducts in solution. These reactions include dechlorination (Figure 5-III) and chlorination (Figure 5-IV). EPFRs can decompose to form cyclopentadienyl radical (Figure 5-V), which then recombines to form derivatives of naphthalene (Figure 5-VI) depending on the metal oxide surface.[17] Hydrogen abstraction from the solvent molecule converts EPFRs to the original molecular precursor, or EPFRs may recombine to form dibenzo-*p*-dioxins (Figure 5-VIII) or dibenzofurans (Figure 5-X). While EPFRs are precursors of dibenzo-*p*-dioxins and dibenzofurans, currently, no studies have measured the fraction of EPFRs that recombines to form these pollutants. A substantial concentration of EPFRs initially exists in solution, which then reacts with other molecular byproducts (e.g., ethers (Figure 5-IX)).[17] Of course, these reaction pathways or the number and type of products presented in Figure 5 are not exhaustive, EPFRs can undergo more reactions that what we outlined here or with what we know so far.

EPFRs in Airborne PM. PM is a complex mixture of liquid and solid components of metals, inorganic, and organic species. Depending on the aerodynamic size, PM is classified into three general modes: coarse, accumulation, and nucleation mode. A particle's aerodynamic size is defined as the size of a particle that has a similar settling velocity to that of a spherical particle.[44] The size distribution of coarse PM ranges between 2.5 and 10 μm; accumulation mode PM ranges <2.5 μm to 100 nm; while the nucleation mode (also called ultrafine particles) are <100 nm. PM's aerodynamic size may indicate its source. Coarse mode PM originates from abrasive physical events such as those from windblown dust, weathering, crushing, and grinding. A large fraction of nucleation and accumulation mode PM originates from combustion sources.

EPFRs in airborne PM is associated primarily with the accumulation and nucleation mode. Measurement of the EPFR concentration from different field campaigns in three cities in different continents indicates that EPFRs are present in the order of 10^{16} to 10^{17} spins/g. Gehling and Dellinger measured the concentration of EPFRs on PM near the Mississippi River in Baton Rouge, Louisiana with a mean concentration of $\sim 4 \times 10^{17}$ spins/g PM.[30] Shaltout and colleagues measured EPFR concentration in Taif, Saudi Arabia with a mean concentration of $\sim 4 \times 10^{16}$ spins/g PM,[45] whereas Arangio and colleagues

DOI: 10.1021/acs.est.7b04439
Environ. Sci. Technol. 2018, 52, 2468−2481

measured EPFR concentration at the rooftop of the Max Planck Institute in Germany to be ~2 × 10^{17} spins/g PM.[46] Arangio and colleagues measured EPFR concentration in different size fraction of PM. Measurements indicated that PM smaller than 56 nm and those larger than 560 nm contained no substantial amount of EPFRs.[46] The highest concentration of EPFRs is at a lower cutoff size of 100 nm.[46] This result is expected as EPFRs are associated with combustion-generated soot particles, which peaks between 100 and 200 nm.[47]

Spin−trapping measurement of short-lived radicals that may result from catalytic cycling of EPFR or reactions among the components in PM revealed that at all size fractions, carbon-centered radicals are the most abundant, whereas $O_2^{\cdot-}$ were the least abundant.[46] Hydroxyl radical contributed 11−31% of the total trapped radical, which appears to be the dominant species for the coarse fraction.[46]

Assuming that 10−50% of PM is organic carbon by mass concentration ($\mu g/m^3$),[7] using the 24-h National Ambient Air Quality Standard (NAAQS) $PM_{2.5}$ concentration of 35 $\mu g/m^3$ and 70% of PM originates from combustion sources,[48] and an EPFR concentration of 10^{10} radical/μg indicates that in airborne PM, EPFRs contribute at least ~2 × 10^{-4}% relative to the organic fraction. While this amount is low, health effects studies in rodents[3,5,49,50] demonstrate significant adverse effects attesting to the potency of EPFRs. The amount of EPFRs adsorbed on PM in different cities are expected to vary depending on the extent of combustion emission sources for that area. We predict that PM in Beijing, China, or New Delhi, India will contain higher EPFR concentration per mass of PM than those of London, UK or Paris, France.

Given the concentration of EPFRs in PM, Gehling, and Dellinger compared it to the amount of EPFRs on cigarette smoke with the average 24 h U.S. NAAQS, which suggests that inhalation of $PM_{2.5}$ containing EPFRs is equivalent to smoking one cigarette every 3 days.[30] However, the amount that enters into the respiratory system may be lower or higher because PM deposits in the different regions of the respiratory tract at varying extent depending on size.[51,52]

PM resulting from primary emission in combustion (including biomass burning) or thermal processing may not be the only source of EPFRs in the atmosphere. SOA may contribute substantially to EPFRs in atmospheric PM. First, SOA constitutes most of the organic fraction in $PM_{2.5}$ that result from the multigenerational oxidation of VOCs[53] or from the multiphase chemistry of VOC-derived oxidation products.[54] Second, SOA constituents are multifunctional monocyclic or polycyclic aromatic products, furans, aldehydes, etc., some of which may be resonance-stabilized and EPFR-like in their molecular structures. Organic components in SOA containing aromatic ring: oxidation products of aromatic VOCs (e.g., benzene, toluene, xylene, and ethylbenzene) and PAHs; naturally occurring organics in tropospheric particles such as retene, 5,6,7,8-tetrahydrocadalene, dehydroabietic acid, calamenene,[55,56] and similar structures are possible candidates to form EPFRs. Third, recent works have shown that isoprene-derived SOA[57−60] and other types of SOA[61,62] induce oxidative stress and inflammation—similar responses elicited by EPFRs. Current knowledge suggests that transition metal-containing particles are required for EPFRs to form. Transition metals constitute a significant component in SOA[63] where they can form complexes with organic species.[64,65] Ascertaining the contribution of SOA as a source of EPFRs requires answering many knowledge gaps. For instance, whether tropospheric temperature is sufficient to drive the reaction, which is lower than those existing in the postcombustion zone or if the reaction can be driven photocatalytically. To date and to our knowledge, no one has measured EPFRs contained in SOA either in ambient atmosphere or in the lab.

Health Effects of EPFRs. Inhalation of atmospheric PM along with the combustion byproducts that are adsorbed on them is implicated in a variety of cardiovascular,[5,49] respiratory,[3] immunological, and lately may be linked to possible neuro-degenerative responses.[66] Here, we refer to EPFRs as persistent free radicals bound to a surrogate PM. The studies presented in this section had used a control surrogate PM that did not contain EPFRs. Toxicological studies in murine (rodents) models have implicated EPFRs with cardiovascular and respiratory dysfunctions;[49] an increased potential for developing asthma;[3] reduced blood supplies and ischemia;[5] and an increased likelihood of influenza infection.[6]

Studies from Cormier and colleagues associate exposure to EPFRs with a variety of diseases as gleaned from numerous in vitro and in vivo studies performed in rodents and some human cells lines.[49] BEAS-2B cells exposed to EPFRs exhibited cytotoxic response.[49] This result correlates with the ability of the EPFRs to amplify cellular oxidative stress leading to a diminished antioxidant defense as well as an increase in lipid peroxidation.[49]

Exposure to a high level of lab-prepared PM that contained EPFRs correlates with the exacerbation of the risk of an asthma attack in infants and children.[4] EPFRs in PM may significantly contribute to this effect. Seven-day-old neonatal rodents exposed to EPFRs develop significant pulmonary inflammation and lung dysfunction (airway hyperactivity).[4] This response correlated with higher levels of oxidative stress in the lungs, altered expression of some proteins associated with oxidative stress, and the regulation of glucocorticoid receptor that is translocated in T-lymphocytes.[4]

In vivo exposure of infant rats to EPFRs results in airway hyper-responsiveness to methacholine, a marker for asthma.[67,68] At high concentration, EPFR exposure induces necrosis; while at low concentration, EPFR exposure leads to a more permeable lysosomal membrane, an elevated level of oxidative stress, and enhanced lipid peroxidation.[67,68] In neonatal rodents that were exposed to EPFRs, their airway epithelial cells transform into mesenchymal cells, which increases the risk of asthma.[67,68]

While early exposure of infants to elevated levels of ambient PM, which should contain EPFRs enhances the risk of developing asthma,[69−71] epidemiological studies suggest that mothers exposed to ambient PM are more likely to have offspring with childhood asthma as well.[50] In utero exposure to EPFRs induces systemic oxidative stress.[72] This reaction enhances postnatal asthma development in the offspring of the exposed mothers compared to nonexposed ones.[72]

Inhalation of EPFRs also alters the phenotype and function of bone marrow-derived dendritic cells and the subsequent T-cell response.[73] EPFRs directly induce dendritic cells to mature, the extent of which is sensitive to particle uptake and the level of oxidative stress induced by the EPFRs.[73] In adult animals, EPFRs induce a phenotypic change in pro-inflammatory cells (Th17) in the lungs, accompanied by a significant formation of pulmonary neutrophilia, which indicate the onset of severe asthma.[73] These data suggest that exposure to EPFRs may contribute to the development and severity of asthma in humans.[73]

DOI: 10.1021/acs.est.7b04439
Environ. Sci. Technol. 2018, 52, 2468−2481

In addition to pulmonary inflammation, EPFRs induce cardiac inflammation.[5] EPFRs decrease left ventricular function before and after ischemia (reduced blood flow), and reperfusion (increased blood flow, I/R) in vivo in male rats, which lead to a decreased systolic and diastolic functions.[5] However, after ischemia, only the systolic function significantly decreased.[5] EPFRs produce inflammation and significantly decrease cardiac function at baseline and after I/R in vivo, suggesting that EPFRs may be a risk factor for cardiac toxicity in healthy individuals and those with ischemic heart disease.[5]

Studies suggest a link between PM and increased severity of respiratory tract infections.[74,75] Aside from respiratory and cardiovascular effects, exposures to elevated levels of EPFRs enhance the severity of virus infection in infant mice.[6] Exposure to EPFRs during infancy led to pulmonary oxidative stress and enhanced the severity of influenza.[6] Mice, less than 7 days old, exposed to EPFRs for seven consecutive days, and then infected with Influenza A virus has significantly enhanced morbidity and decreased survival that is dependent on dose.[6] Reduction of EPFR-induced oxidative stress attenuated these effects.[6] In another study on e-cigarettes, which also contain EPFRs, mice that were infected with *Streptococcus pneumonia* and Influenza A then exposed to e-cigarette vapors exhibit an impaired pulmonary bacterial clearance as well as elevated morbidity from the virus.[76] The combination of uptake of EPFRs and resulting oxidative stress increase morbidity and mortality via a mechanism involving T-regulatory cells.[6]

However, caution is needed to translate these results to human implication because there are no studies directly linking EPFRs to human health effects; only studies of PM that contain EPFRs eliciting human health effects such as those we have observed in rodents and human cell lines exist.

Chemical Basis of EPFR Toxicity. Unlike molecular contaminants, the adverse effects associated with inhaled PM that contain EPFRs arise not only from the molecular byproducts formed when EPFRs recombine, but also because EPFRs catalytically amplify the formation of reactive oxygen species (ROS).[77] The toxic response primarily associated with PM is through the generation of ROS,[78−80] which include hydrogen peroxide, superoxide, and hydroxyl radical, the latter, being the most damaging of all the ROS.[81−84]

Khachatryan and colleagues established the chemical basis of the toxicity of EPFRs in liquid media, which may likely be the mechanism in a biological system.[77] Electron paramagnetic resonance measurement and spin trapping techniques demonstrated that at an incubation time of ∼2 h, a single EPFR generates 10 ROS via catalytic cycling. Figure 6 illustrates the catalytic cycling of superoxide anion radical ($O_2^{\cdot -}$) induce by for a semiquinone-type EPFR. Considering the amount of EPFRs on PM that range from 10^{16} to 10^{17} spins/g PM indicate that a substantial amount of ROS is produced.

In a biological system, and in the presence of biological reducing agents like NADPH, superoxide anion radical can dismutate to hydrogen peroxide (Figure 7-II)).[85] Hydrogen peroxide forms hydroxyl radical via Fenton or Fenton-type reactions (Figure 7-III).[86] Exogenous Fe in PM exist as Fe(III) rather than Fe(II) and are immobilized in PM,[87] and so are other metals, and therefore, inactive toward Fenton/Fenton-type reactions. However, superoxide can attack iron−sulfur cluster proteins, which are present in many biological systems.[88] Once Fe is liberated from these proteins, it is available to participate in Fenton reaction.[88]

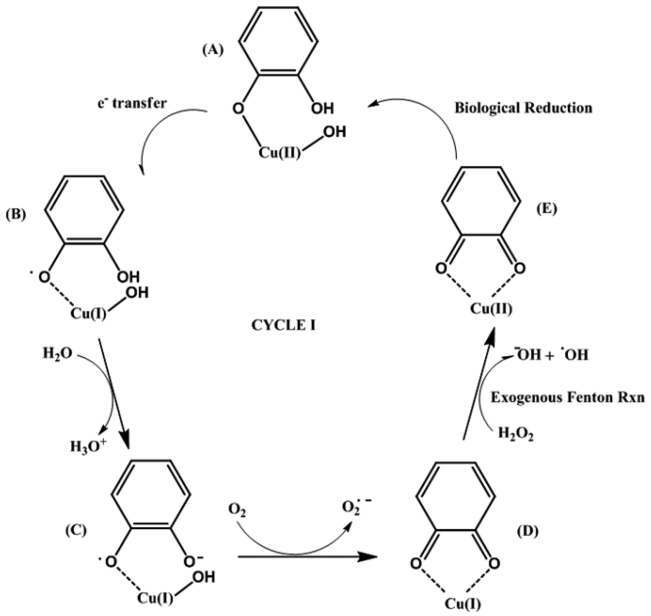

Figure 6. A semiquinone-type radical (C) reduces molecular oxygen to form a superoxide anion radical by catalytic cycling. Superoxide anion radical can dismutate to hydrogen peroxide and produce hydroxyl radical via exogeneous Fenton/Fenton-type reactions. Adapted from Khachatryan et al., 2011 with permission from the American Chemical Society. Copyright 2011.

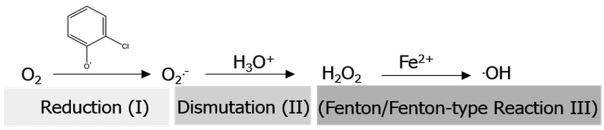

Figure 7. A surface-bound chlorophenoxyl EPFR reduces molecular oxygen to superoxide, which dismutates to hydrogen peroxide and produce hydroxyl radical via exogeneous Fenton/Fenton-type reactions.

EPFR Formation from Unsubstituted Benzene. Based on previous results,[1,18,17,89,90] it appears that the aromatic precursor requires an easily donatable proton, such as those in phenol, or that it should contain electronegative atom such as chlorine to form a chemisorbed species on the surface by eliminating H_2O, HCl, or both. Our earlier studies only used aromatic precursors that contained hydroxy- and chlorine-substituents.[1,18,17,89,90] The hydrogen atoms on benzene are less likely to react with the transition metal oxide surface because such reaction will perturb and diminish benzene's aromaticity. Will an aromatic species without a donatable hydrogen atom (benzene) form EPFRs that are stable and persistent?

Density functional theory (DFT) study by D'Arienzo and colleagues suggests that EPFRs can form from benzene on Cu(II)O.[68] DFT calculation suggests that the benzene ring donates 0.5 e^- to the O atom on the metal oxide surface.[68] In the initial step of formation, O_2 activates the Cu(II)O, which forms an epoxide-like structure with an energy of adsorption of 23.9 kcal/mol.[68] Then, benzene physically interacts with the activated surface, in which the C atom on benzene bonds with the surface O atom on Cu(II)O.[68] Abstraction (transfer) of H atom from the benzene ring forms a phenolate species, and electron transfer forms a phenoxyl radical.[68]

DOI: 10.1021/acs.est.7b04439
Environ. Sci. Technol. 2018, 52, 2468−2481

Experimental validation of the DFT calculation using ~5 nm Cu(II)O nanoparticles supported on a surface generated a broad anisotropic EPR signal that contains unresolved hyperfine coupling interactions.[68] The authors ascribed the EPR signal consistent with a tetragonal symmetry to a d^9-Cu(II) center overlaid to an organic spectrum. The free radical exhibited a *g*-factor of 2.0030, a characteristic of an organic free radical, which the authors assigned to a phenoxyl radical derived from oxidized benzene.[68] However, only a low concentration of EPFRs was formed from benzene[68] compared from those of substituted benzenes.[1] Forming a phenoxyl free radical is less likely since it disrupts the aromaticity of the benzene ring.

The adsorption of benzene did not result in a measurable shift in the X-ray photoelectron spectrum.[68] Although, the author noted a diminished intensity of Cu resonance suggesting the reduction of Cu(II) to Cu(I).[68]

The study did not assess the EPFRs' persistence. A free radical under vacuum does not necessarily translate to a persistent free radical under ambient temperature and pressure. But given the persistence of phenoxyl radical, we expect EPFRs that were formed from benzene to exhibit similar lifetimes as those observed for EPFRs on Cu(II)O in our earlier studies.[1]

■ ALTERNATIVE MECHANISM OF EPFR FORMATION

While the conceptual mechanism described in Figure 2 successfully explains the formation of EPFRs on Cu(II)O, Ni(II)O, $Fe(III)_2O_3$, and $Ti(IV)O_2$ surfaces, this view is inconsistent for EPFRs that are formed over a Zn(II)O surface. During initial work conducted on EPFR formation of Zn(II)O, the question emerged whether EPFRs would form. The *d*-orbitals of Zn(II) are filled; electron distribution within the *d*-orbitals would remain the same even if an aromatic species associates as a high- or low-spin complex. If indeed the one-electron charge-transfer is a key step in forming EPFRs, in the case of Zn(II)O, EPFRs should not form at all because Zn(II) will be reduced to a nonexistent oxidation state, Zn(I). Surprisingly, stable EPFRs form on a Zn(II)O surface.[2] Even more surprising, these EPFRs persist with the longest-known relaxation times to date.[2]

Studies performed over a single Zn(II)O (1010, 0001) crystal using phenol as a molecular precursor by Thibodeaux and colleagues demonstrated that the electron transfers from the Zn(II)O surface toward phenol.[90] Additionally, the adsorption of phenol does not form metallic Zn.[90] These results demonstrate that electron transfer highly depends on band bending.[90] Band bending is the shift in energies of the valence and conduction bands of the material. For Zn(II)O, whether a partial or full charge transfer occurs is unknown. Clearly, more theoretical and experimental studies are needed to understand reactions dictating the formation of phenoxy-type EPFRs on Zn(II)O. These findings contradict the prevailing conceptual model on EPFR formation, and therefore the mechanism presented in Figure 2 cannot be generalized. These results imply that EPFRs can form via other mechanisms.

In the succeeding sections, we present an important research focus on why ENMs may form EPFRs and the conditions at which EPFRs may form. We hypothesize that band bending can facilitate charge transfer easily between an unsupported ENM surface and a molecular adsorbate, depending on size. An important condition is that ENMs must survive and remain intact after incineration to form and stabilize EPFRs. ENMs have lower melting point, hence, are susceptible to physicochemical changes, which may impact the formation of EPFRs. We present findings from previous studies as direct and indirect evidence for the formation of EPFRs on unsupported ENMs.

Role of Band Bending in ENMs on EPFR Formation. Over the past decade, significant progress has been made in understanding the formation and nature of EPFRs. However, large knowledge gaps still exist, for instance, how EPFRs may form on emerging contaminants such as in pristine unsupported ENMs. The prevailing conceptual mechanism assumes that only transition metal oxide surfaces and substituted aromatic structures can react to form EPFRs. The study presented above clearly demonstrates that aromatic structure without substituents (benzene) forms an EPFR as well.[68]

Previous studies mimic the formation of EPFRs over nanoparticles supported on a large micrometer-sized surface,[1,17,18] which simulated EPFR formation on surfaces of incidental nanoparticles. Will EPFRs form on particles that are unsupported pristine engineered nanoparticles? We hypothesize that because the band gap for ENMs exhibit size-dependence and thermally excited electrons may easily cross the band gap, some ENMs, depending on size, electronic, and chemical properties may form EPFRs. Therefore, ENMs may form EPFRs with properties that potentially differ from those observed over incidental nanoparticles (those supported on surfaces)—more importantly, their persistence. The insight obtained from the previous study that electrons can move in both directions (nanoparticle-to-organic moiety and from the organic moiety-to-nanoparticle) implies two important consequences. First, ENMs that are unsupported on an insulating or a semiconducting layer (i.e., the absence of Schottky contact) can form EPFRs. Thermal perturbation, as in the case of incineration or thermal treatment, can enhance electron transfer, for instance, an electron traversing a band gap and an electron moving between the energy levels of molecular orbitals of a donor/acceptor molecule.[91] Second, nanoparticles with surface chemistry other than that of transition metals (i.e., carbonaceous nanoparticles) can form EPFRs if the nanoparticles survive incineration and exit into the postcombustion zone intact. Evidence for the persistence of carbonaceous nanoparticles is discussed in the next section.

As demonstrated by Thibodeaux and colleagues, band bending dictates the movement of an electron on Zn(II)O surface to phenol.[90] Using the equation developed by Alberry and Bartlett for a large spherical semiconductor particle with radius $r_o \gg D$, where D is the depletion layer (the region without charge carriers). Zhang and Yates[91] approximated that the extent of band bending follows:

$$V_{BB}(r_o) = \frac{eN_dD^2}{2\varepsilon_r\varepsilon_o} \quad (1)$$

For a small particle, in which $r_o < \sqrt{3D}$, the surface band bending is

$$V_{BB}(r_o) = \frac{eN_d{r_o}^2}{6\varepsilon_r\varepsilon_o} \quad (2)$$

In these equations, V_{BB} is the magnitude of band bending, e is the electronic charge, N_d is the dopant concentration, r_o is the radius of the particle, ε_r is the relative dielectric constant, and ε_o is the permittivity of vacuum.

DOI: 10.1021/acs.est.7b04439
Environ. Sci. Technol. 2018, 52, 2468−2481

For pristine nanoparticles (i.e., undoped), this approximation indicates that V_{BB} for small particle depends on r_o and ε_r. V_{BB} will increase with larger particle size. An extremely small nanoparticle will induce small V_{BB} or may even be negligible[92,93] as illustrated in Figure 8. A nanoparticle with a low ε_r will increase V_{BB}. For instance, V_{BB} for Zn(II)O will be higher than Ti(IV)O_2 because of the lower ε_r value for Zn(II)O.[94] Different surfaces induce different electric fields affecting the lifetime of the electron, and hence the lifetime of the free radicals. The lower dielectric constant for Zn(II)O compared to Ti(IV)O_2[94] may explain the slightly longer lifetimes of EPFRs generated over Zn(II)O[2] than for Ti(IV)O_2.[24] Although, EPFRs bound to both metals have a similar order of persistence and are among the most persistent.[2,24]

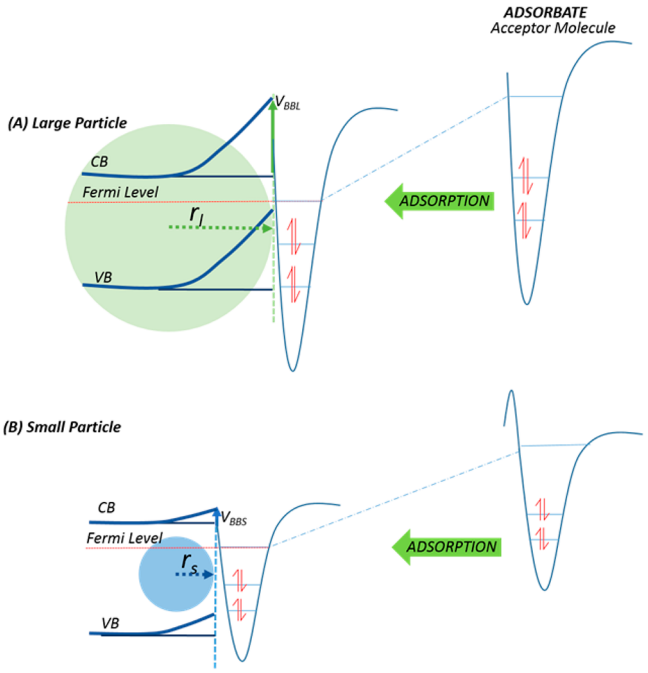

Figure 8. Band bending of a donor molecule for small and large particles. CB and VB are the conduction band and the valence band, respectively. V_{BBS} and V_{BBL} refer to the magnitude of band bending for small and large particles, respectively. A small particle has a lower magnitude of V_{BB} whereas a larger particle has a higher magnitude V_{BB}. Adapted from Albery, 1984 and Zhang and Yates, 2012 with permission from the American Chemical Society. Copyright 1984 and 2012.

Charge-transfer between a nanoparticle and an adsorbate depends on (1) the excitation of the charge carrier from the valence band to the conduction band and (2) the extent and direction of band bending (Figure 8). Both properties depend on particle size.[95] The presence of a donor−acceptor molecule on the surface affects the probability of charge-transfer from the surface to the adsorbate, depending on direction and extent of band bending.[96] Molecules that donate electrons promote downward band bending,[96] whereas those that accept electrons promote upward band bending. Figure 8 illustrates upward band bending (V_{BBS} and V_{BBL}) induced by a donor molecule. As shown in Figure 8, the adsorption of a molecule on the surface of the particle lowers the energy of the lowest energy unoccupied molecular orbitals of the acceptor molecule to near the Fermi level (the energy level for a collection of surface electrons at absolute zero).

Band gap energy is the energy difference between the conduction and valence bands. For an ENM with a band gap energy similar to that of semiconductor (~4 eV),[97] electrons in the valence band can be excited thermally to the conduction band at a sufficiently high temperature. Band gap energy decreases as a function of temperature as in the case of silicon.[98] Some ENMs such as C_{60}-fullerene and single-walled carbon nanotubes have band gap energies of 1.9 eV[99] and <0.1 eV,[100] respectively, which are well below those of semiconductors. For nanoparticles, band gap energy increases with decreasing particle size (r) by $1/r^2$.[97] However, if the band gap energy for a small nanoparticle is considerably higher (but lower than the bulk material), the high temperature even at the relatively low temperature of the cool zone of combustion may be sufficient to enhance the probability of charge transfer into the conduction band. We hypothesize that charge transfer can occur either to the nanoparticle or to the organic molecule for small silica nanoparticles that can form and stabilize EPFRs. Therefore, ENMs may generate higher concentration of EPFRs

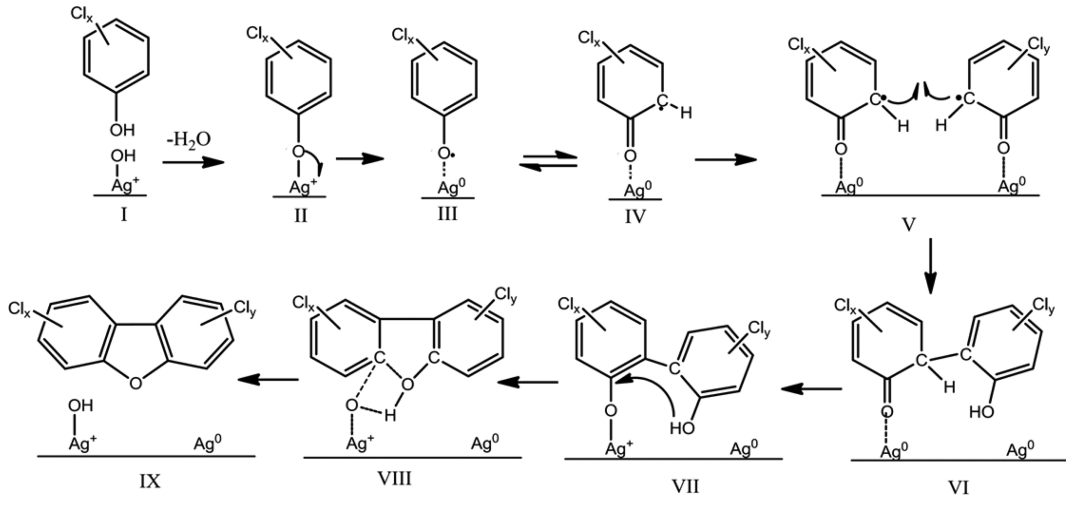

Figure 9. Hypothesized mechanism of the formation of dibenzofuran from recombination of a surface-bound free radical on a silver oxide surface. Adapted from Vejerano et al., 2013 with permission from the American Chemical Society. Copyright 2013.

DOI: 10.1021/acs.est.7b04439
Environ. Sci. Technol. 2018, 52, 2468−2481

compared to incidental nanoparticles even at a lower temperature.

Emission of Carbonaceous Nanoparticles During Thermal Treatment. If carbonaceous nanoparticles—fullerenes and carbon nanotubes—are to form EPFRs, they should first survive incineration. In our study on the incineration of ENMs with solid wastes, a significant fraction of C_{60}-fullerenes survived incineration at 850 °C.[16] In isolation, C_{60}-fullerene completely oxidizes at 500 °C.[101] Extensive penetration of C_{60}-fullerenes into the matrix as well as polycyclic aromatic hydrocarbons and soot effectively coating C_{60}-fullerenes render them less susceptible to oxidation.[16] Aside from fullerenes, single-walled carbon nanotubes incorporated in polymer matrices are released unmodified both as isolated or bundled fibers when thermally treated.[102] Many ENMs are incorporated in polymer matrices, in which we expect a greater fraction of them to remain intact even after incineration.[15] These results suggest that ENMs that survive intact after incineration have the potential to form EPFRs.

EPFR Formation on ENMs. Our earlier work on the incineration of ENMs suggests the potential of ENMs to form EPFRs over their surfaces. While we did not measure the concentration of EPFRs formed during the incineration of ENMs with surrogate wastes, the presence of a high concentration of dibenzofurans, but not dibenzo-*p*-dioxins, suggests that some ENMs, notably silver and anatase-Ti(IV)O_2 favor the formation of surface-bound free radicals.[13] The formation of dibenzofurans proceeds through the recombination of surface-bound free radicals (Langmuir−Hinshelwood mechanism), whereas a gas-phase molecule can recombine with a surface-bound radical to form dibenzo-*p*-dioxins (Eley−Rideal mechanism).[30,84]

Figure 9 illustrates the recombination of two carbon-centered radicals (Figure 9-IV) to form chlorinated dibenzofuran (Figure 9-IX) over the surface of silver.[16] Ti(IV)O_2 may undergo a similar mechanism with the reduction of Ti^{4+} to Ti^{3+} and subsequent formation of a surface-bound radical that recombines to dibenzofuran.[16] The high emission of dibenzofurans indicates that Ag and anatase-Ti(IV)O_2 form high amount of EPFRs from the combined effect of the high specific surface area and the type of transition metal. In the case of Ag, an indirect evidence of EPFR formation is that the measured *d*-spacing of 2.01 Å agrees with the distance for an Ag−O system (2.04 Å).[103] Additionally, the *d*-spacing of 4.01 is close to the *d*-spacing of 4.09 Å, which suggests chemisorbed oxygen on the surface of Ag.[103]

In our previous studies, we did not observe EPFRs forming on micrometer-size silica particles that we used to support the nanoparticles, presumably because of the large band gap energy in bulk silica (~9.0 eV).[104] However, for a silica nanoparticle, the band gap energy may be lower than that of bulk silica, which then may form EPFRs. Additionally, when a donor or acceptor molecule interacts with a smaller particle (e.g., nanoparticle), this interaction lowers the energy of the empty molecular orbital inducing band bending, as observed for phenol.[91,105] Thus, smaller particles are more likely to facilitate charge-transfer between the nanoparticle's surface and into the energy level of a donor−acceptor molecule. Patterson and colleagues demonstrated that 18 nm Zn(II)O nanoparticles form EPFRs even at room temperature[89]—the lowest temperature in which EPFRs have been observed to form.

Impact of the Physico-Chemical Changes of ENMs on EPFR Formation. Transformations of ENMs can influence their effects on pollutant formation. Melting points of nanoparticles decrease with particle size.[106,107] Thus, when incinerated or thermally treated, nanoparticles are susceptible to changes in size, morphology, and crystalline phases. Our earlier studies suggest that some ENMs, for instance, Ag and CdSe/ZnS quantum dots became larger than the original nanoparticles.[16] Incinerated ENMs may result in gross changes in size and morphology.[16] Although some ENMs may not display such changes, for some crystalline ENMs, phase transition may occur.[16] Phase transition for some bulk crystalline compounds occurs well below the temperature used in conventional incinerators, less so for ENMs because of their small particle size and higher surface energies.[108,109] For some solids; phase transition drastically alters their properties such as optical and catalytic activities.[110] Anatase-Ti(IV)O_2 is more photocatalytically active compared to its rutile phase because charge carriers that are buried deeper in the bulk structure of anatase-Ti(IV)O_2 nanoparticle can be excited easily to participate in surface reactions compared to rutile-Ti(IV)-O_2.[110] Depending on size, the initiation transition temperature for anatase-Ti(IV)O_2 (520 to 850 °C)[111,112] to transform into its thermodynamically more stable rutile phase is well below those used in incinerators. Different crystal structures may affect EPFR formation at varying extents. For instance, the formation of polycrystalline intermetallic phases of Pd/Sn nanoparticles diminished the catalytic activity of the face-centered cubic phase in oxidizing carbon monoxide.[113] Photocatalytic and thermal catalytic activities of ENMs with different phases might have higher activity than those containing a pure phase.[114] For instance, Degussa-P25 TiO_2, which contains both rutile and anatase phases exhibits a higher catalytic activity compared to the pure phases alone.[114] Conversion of ENMs and the coexistence of multiple crystalline phases may enhance or decrease the formation of EPFRs.

SUMMARY AND OUTLOOK

EPFRs are formed when combustion byproducts interact with transition metal oxide surface at the surface-catalysis cool combustion zone. Unlike previously identified atmospheric free radicals that typically have lifetimes of only a fraction of a second, EPFRs are unique because of their extreme persistence on the order of several minutes to months. Therefore, EPFRs comprise a class of pollutant with important environmental and health implications. EPFRs in airborne PM are associated with the accumulation and nucleation mode and exist in sufficient concentration to induce adverse health effects observed by us and others in animal and cell models. The earlier conceptual thought on the formation of EPFRs is that they form through a series of steps: physisorption, chemisorption, and electron transfer.

To date, toxicological studies have implicated PM containing EPFRs in a variety of cardiovascular and respiratory dysfunctions and increased susceptibility to influenza infection in vulnerable populations. Toxicological effects of EPFRs arise not only from the molecular byproducts that result from the recombination of EPFRs and subsequent conversion to molecular byproducts but more importantly from ROS that are generated from the catalytic cycling of EPFRs.

Over the past decade, significant progress has been made in understanding the nature of EPFRs. However, significant knowledge gaps still exist. Earlier laboratory studies on EPFRs have been constrained only on surfaces of transition metal oxides and molecular precursors containing substituted

DOI: 10.1021/acs.est.7b04439
Environ. Sci. Technol. 2018, 52, 2468−2481

aromatic structures synthesized above 150 °C. Moreover, these studies mimic EPFR formation on nanoparticles that are supported on a larger particle. Recent studies demonstrated that EPFRs can form from an aromatic molecule without substituents; and electron can transfer from the metal surface to the organic molecule—contrary to the prevailing conceptual thought that electron transfer proceeds exclusively from an organic molecule to the surface of a transition metal oxide. These results imply that EPFRs can form via other mechanisms.

ENMs have lower band gap energy compared to their bulk counterpart; and the extent of band bending for ENMs depends on size. Therefore, ENMs are likely to produce EPFRs. Nonmetallic ENMs (fullerenes, carbon nanotubes, or nano-silica) can potentially form EPFRs as they exhibit "metallic" character because of their band gap energies. Because nanoparticles exhibit lower melting points, they are susceptible to changes in size, morphology, and crystalline structure during high-temperature and oxidative treatment, which may influence EPFR formation. Because of band bending, and the nature of the adsorbate, we hypothesize that the formation of EPFRs may be more common than initially thought, and that EPFRs can form on surfaces other than those on transition metal oxides.

Currently, no extensive studies have been conducted on the role of ENMs that are unsupported on a larger particle in forming EPFRs. The surface, physical, and chemical properties of ENMs may affect the type, concentration, and properties of EPFR that may differ substantially than those formed over nanoparticles that are supported on a larger particle. Answering research questions regarding EPFRs and ENMs will generate data that will help mitigate future adverse impacts of ENMs. As emerging environmental contaminants, understanding the role of ENMs in forming EPFRs is critical to fully assess the environmental and health risk associated with atmospheric PM.

AUTHOR INFORMATION

Corresponding Author

*Phone: (803) 777 6360; e-mail: vejerano@mailbox.sc.edu.

ORCID

Eric P. Vejerano: 0000-0002-6737-9057

Lavrent Khachatryan: 0000-0002-8067-7964

Notes

The authors declare no competing financial interest.

ACKNOWLEDGMENTS

We thank the National Institute of Environmental Health Sciences for continuously funding the studies on EPFRs and the National Science Foundation. EPV was supported by an NSF EPSCoR RII-Track IV grant 1738337. This work was supported by NIEHS Superfund grant to SAC and SL (P42ES013648) and NIEHS grant to SAC (R01ES015050).

DEDICATION

We dedicate this paper to the memory of Dr. Barry H. Dellinger, whose pioneering research on EPFRs has inspired us all to continue his work.

REFERENCES

(1) Lomnicki, S.; Truong, H.; Vejerano, E.; Dellinger, B. Copper oxide-based model of persistent free radical formation on combustion-derived particulate matter. *Environ. Sci. Technol.* **2008**, *42* (13), 4982–4988.

(2) Vejerano, E.; Lomnicki, S.; Dellinger, B. Lifetime of combustion-generated environmentally persistent free radicals on Zn(II)O and other transition metal oxides. *J. Environ. Monit.* **2012**, *14* (10), 2803.

(3) Fahmy, B.; Ding, L.; You, D.; Lomnicki, S.; Dellinger, B.; Cormier, S. A. In vitro and in vivo assessment of pulmonary risk associated with exposure to combustion generated fine particles. *Environ. Toxicol. Pharmacol.* **2010**, *29* (2), 173–182.

(4) Balakrishna, S.; Saravia, J.; Thevenot, P.; Ahlert, T.; Lomniki, S.; Dellinger, B.; Cormier, S. A. Environmentally persistent free radicals induce airway hyperresponsiveness in neonatal rat lungs. *Part. Fibre Toxicol.* **2011**, *8* (1), 11.

(5) Lord, K.; Moll, D.; Lindsey, J. K.; Mahne, S.; Raman, G.; Dugas, T.; Cormier, S.; Troxlair, D.; Lomnicki, S.; Dellinger, B. Environmentally persistent free radicals decrease cardiac function before and after ischemia/reperfusion injury in vivo. *J. Recept. Signal Transduction Res.* **2011**, *31* (2), 157–167.

(6) Lee, G. I.; Saravia, J.; You, D.; Shrestha, B.; Jaligama, S.; Hebert, V. Y.; Dugas, T. R.; Cormier, S. A. Exposure to combustion generated environmentally persistent free radicals enhances severity of influenza virus infection. *Part. Fibre Toxicol.* **2014**, *11* (1), 57.

(7) Seinfeld, J. H.; Pandis, S. N. *Atmospheric Chemistry and Physics: From Air Pollution to Climate Change*, 3rd ed.; John Wiley & Sons: Hoboken, NJ, 2016.

(8) Roco, M. C.; Mirkin, C. A.; Hersam, M. C. Nanotechnology research directions for societal needs in 2020: Summary of international study. *J. Nanopart. Res.* **2011**, *13* (3), 897–919.

(9) Keller, A. A.; Lazareva, A. Predicted releases of engineered nanomaterials: from global to regional to local. *Environ. Sci. Technol. Lett.* **2014**, *1* (1), 65–70.

(10) Maynard, A. D. Nanotechnology: Assessing the risks. *Nano Today* **2006**, *1* (2), 22–33.

(11) Kim, S. H.; Ahn, S.-Y.; Kwak, S.-Y. Suppression of dioxin emission in incineration of poly(vinyl chloride) (PVC) as hybridized with titanium dioxide (TiO_2) nanoparticles. *Appl. Catal., B* **2008**, *79* (3), 296–305.

(12) Font, R.; Gálvez, A.; Moltó, J.; Fullana, A.; Aracil, I. Formation of polychlorinated compounds in the combustion of PVC with iron nanoparticles. *Chemosphere* **2010**, *78* (2), 152–159.

(13) Vejerano, E. P.; Holder, A. L.; Marr, L. C. Emissions of polycyclic aromatic hydrocarbons, polychlorinated dibenzo-p-dioxins, and dibenzofurans from incineration of nanomaterials. *Environ. Sci. Technol.* **2013**, *47* (9), 4866–4874.

(14) Sotiriou, G. A.; Singh, D.; Zhang, F.; Wohlleben, W.; Chalbot, M.-C. G.; Kavouras, I. G.; Demokritou, P. An integrated methodology for the assessment of environmental health implications during thermal decomposition of nano-enabled products. *Environ. Sci.: Nano* **2015**, *2* (3), 262–272.

(15) Sotiriou, G. A.; Singh, D.; Zhang, F.; Chalbot, M.-C. G.; Spielman-Sun, E.; Hoering, L.; Kavouras, I. G.; Lowry, G. V.; Wohlleben, W.; Demokritou, P. Thermal decomposition of nano-enabled thermoplastics: Possible environmental health and safety implications. *J. Hazard. Mater.* **2016**, *305*, 87–95.

(16) Vejerano, E. P.; Leon, E. C.; Holder, A. L.; Marr, L. C. Characterization of particle emissions and fate of nanomaterials during incineration. *Environ. Sci.: Nano* **2014**, *1* (2), 133–143.

(17) Vejerano, E.; Lomnicki, S.; Dellinger, B. Formation and stabilization of combustion-generated environmentally persistent free radicals on an $Fe(III)_2O_3$/silica surface. *Environ. Sci. Technol.* **2011**, *45* (2), 589–594.

(18) Vejerano, E.; Lomnicki, S. M.; Dellinger, B. Formation and stabilization of combustion-generated, environmentally persistent radicals on Ni(II)O supported on a silica surface. *Environ. Sci. Technol.* **2012**, *46* (17), 9406–9411.

(19) dela Cruz, A. L. N.; Gehling, W.; Lomnicki, S.; Cook, R.; Dellinger, B. Detection of environmentally persistent free radicals at a Superfund wood treating site. *Environ. Sci. Technol.* **2011**, *45* (15), 6356–6365.

(20) Cruz, A. L. N. dela; Cook, R. L.; Lomnicki, S. M.; Dellinger, B. Effect of low temperature thermal treatment on soils contaminated

DOI: 10.1021/acs.est.7b04439
Environ. Sci. Technol. 2018, 52, 2468–2481

with pentachlorophenol and environmentally persistent free radicals. *Environ. Sci. Technol.* **2012**, *46* (11), 5971−5978.
(21) Nwosu, U. G.; Roy, A.; dela Cruz, A. L. N.; Dellinger, B.; Cook, R. Formation of environmentally persistent free radical (EPFR) in iron (III) cation-exchanged smectite clay. *Env. Sci. Process. Impacts* **2016**, *18* (1), 42−50.
(22) Jia, H.; Nulaji, G.; Gao, H.; Wang, F.; Zhu, Y.; Wang, C. Formation and stabilization of environmentally persistent free radicals induced by the interaction of anthracene with Fe(III)-modified clays. *Environ. Sci. Technol.* **2016**, *50* (12), 6310−6319.
(23) Altarawneh, M.; Dlugogorski, B. Z. Formation of dibenzofuran, dibenzo-p-dioxin and their hydroxylated derivatives from catechol. *Phys. Chem. Chem. Phys.* **2014**, *17* (3), 1822−1830.
(24) Patterson, M. C.; Keilbart, N. D.; Kiruri, L. W.; Thibodeaux, C. A.; Lomnicki, S.; Kurtz, R. L.; Poliakoff, E. D.; Dellinger, B.; Sprunger, P. T. EPFR formation from phenol adsorption on Al_2O_3 and TiO_2: EPR and EELS studies. *Chem. Phys.* **2013**, *422*, 277−282.
(25) Ingram, D. J. E.; Tapley, J. G.; Jackson, R.; Bond, R. L.; Murnaghan, A. R. Paramagnetic resonance in carbonaceous solids. *Nature* **1954**, *174* (4434), 797−798.
(26) Lyons, M. J.; Spence, J. B. Environmental free radicals. *Br. J. Cancer* **1960**, *14* (4), 703−708.
(27) Pryor, W. A.; Terauchi, K.; Davis, W. H. Electron spin resonance (ESR) study of cigarette smoke by use of spin trapping techniques. *Environ. Health Perspect.* **1976**, *16*, 161−176.
(28) Pryor, W. A.; Squadrito, G. L. The chemistry of peroxynitrite: A product from the reaction of nitric oxide with superoxide. *Am. J. Physiol.* **1995**, *268* (5Pt 1), L699−722.
(29) Squadrito, G. L.; Cueto, R.; Dellinger, B.; Pryor, W. A. Quinoid redox cycling as a mechanism for sustained free radical generation by inhaled airborne particulate matter. *Free Radical Biol. Med.* **2001**, *31* (9), 1132−1138.
(30) Gehling, W.; Dellinger, B. Environmentally persistent free radicals and their lifetimes in PM2.5. *Environ. Sci. Technol.* **2013**, *47* (15), 8172−8178.
(31) Dellinger, B.; Pryor, W. A.; Cueto, R.; Squadrito, G. L.; Hegde, V.; Deutsch, W. A. Role of free radicals in the toxicity of airborne fine particulate matter. *Chem. Res. Toxicol.* **2001**, *14* (10), 1371−1377.
(32) *The Environment: Challenges for the Chemical Sciences in the 21st Century*; National Academies Press: Washington, D.C., 2003; https://www.nap.edu/read/10803/Chapter/1.
(33) Cormier, S. A.; Lomnicki, S.; Backes, W.; Dellinger, B. Origin and health impacts of emissions of toxic by-products and fine particles from combustion and thermal treatment of hazardous wastes and materials. *Environ. Health Perspect.* **2006**, *114* (6), 810−817.
(34) Okeson, C. D.; Riley, M. R.; Fernandez, A.; Wendt, J. O. L. Impact of the composition of combustion generated fine particles on epithelial cell toxicity: Influences of metals on metabolism. *Chemosphere* **2003**, *51* (10), 1121−1128.
(35) Alderman, S. L.; Farquar, G. R.; Poliakoff, E. D.; Dellinger, B. An infrared and X-ray spectroscopic study of the reactions of 2-chlorophenol, 1,2-dichlorobenzene, and chlorobenzene with model CuO/silica fly ash surfaces. *Environ. Sci. Technol.* **2005**, *39* (19), 7396−7401.
(36) Farquar, G. R.; Alderman, S. L.; Poliakoff, E. D.; Dellinger, B. X-ray spectroscopic studies of the high temperature reduction of Cu(II) O by 2-chlorophenol on a simulated fly ash surface. *Environ. Sci. Technol.* **2003**, *37* (5), 931−935.
(37) Assaf, N. W.; Altarawneh, M.; Oluwoye, I.; Radny, M.; Lomnicki, S. M.; Dlugogorski, B. Z. Formation of environmentally persistent free radicals on α-Al_2O_3. *Environ. Sci. Technol.* **2016**, *50* (20), 11094−11102.
(38) Altarawneh, M.; Radny, M. W.; Smith, P. V.; Mackie, J. C.; Kennedy, E. M.; Dlugogorski, B. Z.; Soon, A.; Stampfl, C. A first-principles density functional study of chlorophenol adsorption on Cu_2O(110):CuO. *J. Chem. Phys.* **2009**, *130* (18), 184505.
(39) Lomnicki, S.; Dellinger, B. A detailed mechanism of the surface-mediated formation of PCDD/F from the oxidation of 2-chlorophenol on a CuO/silica surface. *J. Phys. Chem. A* **2003**, *107* (22), 4387−4395.
(40) Dellinger, B.; Lomnicki, S.; Khachatryan, L.; Maskos, Z.; Hall, R. W.; Adounkpe, J.; McFerrin, C.; Truong, H. Formation and stabilization of persistent free radicals. *Proc. Combust. Inst.* **2007**, *31* (1), 521−528.
(41) Lichtveld, K. M.; Ebersviller, S. M.; Sexton, K. G.; Vizuete, W.; Jaspers, I.; Jeffries, H. E. *In vitro* exposures in diesel exhaust atmospheres: Resuspension of PM from filters versus direct deposition of PM from air. *Environ. Sci. Technol.* **2012**, *46* (16), 9062−9070.
(42) Vejerano, E. W. P. Formation and stabilization of combustion-generated environmentally persistent free radicals on transition metal oxides supported on silica. Ph.D. Dissertation, Louisiana State University, Baton Rouge, LA, 2011.
(43) Truong, H.; Lomnicki, S.; Dellinger, B. Potential for misidentification of environmentally persistent free radicals as molecular pollutants in particulate matter. *Environ. Sci. Technol.* **2010**, *44* (6), 1933−1939.
(44) Hind, W. C. *Aerosol Technology: Properties, Behavior, and Measurement of Airborne Particles*, 2nd ed.; John Wiley & Sons: Hoboken, NJ, 1999.
(45) Shaltout, A. A.; Boman, J.; Shehadeh, Z. F.; Al-Malawi, D. R.; Hemeda, O. M.; Morsy, M. M. Spectroscopic investigation of PM2.5 collected at industrial, residential and traffic sites in Taif, Saudi Arabia. *J. Aerosol Sci.* **2015**, *79*, 97−108.
(46) Arangio, A. M.; Tong, H.; Socorro, J.; Pöschl, U.; Shiraiwa, M. Quantification of environmentally persistent free radicals and reactive oxygen species in atmospheric aerosol particles. *Atmos. Chem. Phys.* **2016**, *16* (20), 13105−13119.
(47) Bond, T. C.; Doherty, S. J.; Fahey, D. W.; Forster, P. M.; Berntsen, T.; DeAngelo, B. J.; Flanner, M. G.; Ghan, S.; Kärcher, B.; Koch, D. Bounding the role of black carbon in the climate system: A scientific assessment: Black Carbon in the Climate System. *J. Geophys. Res. Atmospheres* **2013**, *118* (11), 5380−5552.
(48) Cass, G. R.; Hughes, L. A.; Bhave, P.; Kleeman, M. J.; Allen, J. O.; Salmon, L. G. The chemical composition of atmospheric ultrafine particles. *Philos. Trans. R. Soc., A* **2000**, *358* (1775), 2581−2592.
(49) Balakrishna, S.; Lomnicki, S.; McAvey, K. M.; Cole, R. B.; Dellinger, B.; Cormier, S. A. Environmentally persistent free radicals amplify ultrafine particle mediated cellular oxidative stress and cytotoxicity. *Part. Fibre Toxicol.* **2009**, *6* (1), 11.
(50) Lee, A.; Leon Hsu, H.-H.; Mathilda Chiu, Y.-H.; Bose, S.; Rosa, M. J.; Kloog, I.; Wilson, A.; Schwartz, J.; Cohen, S.; Coull, B. A. Prenatal fine particulate exposure and early childhood asthma: Effect of maternal stress and fetal gender. *J. Allergy Clin. Immunol.* **2017**, DOI: 10.1016/j.jaci.2017.07.017.
(51) Cassee, F.; Muijser, H.; Duistermaat, E.; Freijer, J.; Geerse, K.; Marijnissen, J.; Arts, J. Particle size-dependent total mass deposition in lungs determines inhalation toxicity of cadmium chloride aerosols in rats. Application of a multiple path dosimetry model. *Arch. Toxicol.* **2002**, *76* (5−6), 277−286.
(52) Martins, V.; Cruz Minguillón, M.; Moreno, T.; Querol, X.; de Miguel, E.; Capdevila, M.; Centelles, S.; Lazaridis, M. Deposition of aerosol particles from a subway microenvironment in the human respiratory tract. *J. Aerosol Sci.* **2015**, *90*, 103−113.
(53) Kroll, J. H.; Seinfeld, J. H. Chemistry of secondary organic aerosol: Formation and evolution of low-volatility organics in the atmosphere. *Atmos. Environ.* **2008**, *42* (16), 3593−3624.
(54) Nozière, B.; Kalberer, M.; Claeys, M.; Allan, J.; D'Anna, B.; Decesari, S.; Finessi, E.; Glasius, M.; Grgić, I.; Hamilton, J. F.; et al. The molecular identification of organic compounds in the atmosphere: State of the art and challenges. *Chem. Rev.* **2015**, *115* (10), 3919−3983.
(55) Simoneit, B. R. T.; Cox, R. E.; Standley, L. J. Organic matter of the troposphere—IV. Lipids in harmattan aerosols of Nigeria. *Atmos. Environ.* **1988**, *22* (5), 983−1004.
(56) Simoneit, B. R. T. Organic matter of the troposphere — V: Application of molecular marker analysis to biogenic emissions into the troposphere for source reconciliations. *J. Atmos. Chem.* **1989**, *8* (3), 251−275.

DOI: 10.1021/acs.est.7b04439
Environ. Sci. Technol. 2018, 52, 2468−2481

(57) Arashiro, M.; Lin, Y.-H.; Sexton, K. G.; Zhang, Z.; Jaspers, I.; Fry, R. C.; Vizuete, W. G.; Gold, A.; Surratt, J. D. *In vitro* exposure to isoprene-derived secondary organic aerosol by direct deposition and its effects on COX-2 and IL-8 gene expression. *Atmos. Chem. Phys.* **2016**, *16* (22), 14079−14090.
(58) Kramer, A. J.; Rattanavaraha, W.; Zhang, Z.; Gold, A.; Surratt, J. D.; Lin, Y.-H. Assessing the oxidative potential of isoprene-derived epoxides and secondary organic aerosol. *Atmos. Environ.* **2016**, *130* (SupplementC), 211−218.
(59) Lin, Y. H.; Arashiro, M.; Martin, E.; Chen, Y.; Zhang, Z.; Sexton, K. G.; Gold, A.; Jaspers, I.; Fry, R. C.; Surratt, J. D. Isoprene-derived secondary organic aerosol induces the expression of oxidative stress response genes in human lung cells. *Environ. Sci. Technol. Lett.* **2016**, *3* (6), 250−254.
(60) Lin, Y.-H.; Arashiro, M.; Clapp, P. W.; Cui, T.; Sexton, K. G.; Vizuete, W.; Gold, A.; Jaspers, I.; Fry, R. C.; Surratt, J. D. Gene expression profiling in human lung cells exposed to isoprene-derived secondary organic aerosol. *Environ. Sci. Technol.* **2017**, *51* (14), 8166−8175.
(61) Tuet, W. Y.; Chen, Y.; Fok, S.; Champion, J. A.; Ng, N. L. Inflammatory responses to secondary organic aerosols (SOA) generated from biogenic and anthropogenic precursors. *Atmos. Chem. Phys.* **2017**, *17* (18), 11423−11440.
(62) Tuet, W. Y.; Chen, Y.; Xu, L.; Fok, S.; Gao, D.; Weber, R. J.; Ng, N. L. Chemical oxidative potential of secondary organic aerosol (SOA) generated from the photooxidation of biogenic and anthropogenic volatile organic compounds. *Atmos. Chem. Phys.* **2017**, *17* (2), 839−853.
(63) Chu, B.; Liggio, J.; Liu, Y.; He, H.; Takekawa, H.; Li, S.-M.; Hao, J. Influence of metal-mediated aerosol-phase oxidation on secondary organic aerosol formation from the ozonolysis and OH-oxidation of α-pinene. *Sci. Rep.* **2017**, *7*, 40311.
(64) Spokes, L. J.; Lucia, M.; Campos, A. M.; Jickells, T. D. The role of organic matter in controlling copper speciation in precipitation. *Atmos. Environ.* **1996**, *30* (23), 3959−3966.
(65) Okochi, H.; Brimblecombe, P. Potential trace metal-organic complexation in the atmosphere. *Sci. World J.* **2002**, *2*, 767−786.
(66) Maher, B. A.; Ahmed, I. A. M.; Karloukovski, V.; MacLaren, D. A.; Foulds, P. G.; Allsop, D.; Mann, D. M. A.; Torres-Jardón, R.; Calderon-Garciduenas, L. Magnetite pollution nanoparticles in the human brain. *Proc. Natl. Acad. Sci. U. S. A.* **2016**, *113* (39), 10797−10801.
(67) Thevenot, P. T.; Saravia, J.; Jin, N.; Giaimo, J. D.; Chustz, R. E.; Mahne, S.; Kelley, M. A.; Hebert, V. Y.; Dellinger, B.; Dugas, T. R. Radical-containing ultrafine particulate matter initiates epithelial-to-mesenchymal transitions in airway epithelial cells. *Am. J. Respir. Cell Mol. Biol.* **2013**, *48* (2), 188−197.
(68) D'Arienzo, M.; Gamba, L.; Morazzoni, F.; Cosentino, U.; Greco, C.; Lasagni, M.; Pitea, D.; Moro, G.; Cepek, C.; Butera, V. Experimental and theoretical investigation on the catalytic generation of environmentally persistent free radicals from benzene. *J. Phys. Chem. C* **2017**, *121* (17), 9381−9393.
(69) Respiratory Effects in Children from Exposure to Secondhand Smoke. In *The Health Consequences of Involuntary Exposure to Tobacco Smoke*, A Report of the Surgeon General; Office on Smoking and Health; Centers for Disease Control and Prevention: Atlanta, GA, 2006.
(70) *Effects of Air Pollution on Children's Health and Development*; http://www.euro.who.int/__data/assets/pdf_file/0010/74728/E86575.pdf.
(71) Schultz, E. S.; Litonjua, A. A.; Melén, E. Effects of long-term exposure to traffic-related air pollution on lung function in children. *Curr. Allergy Asthma Rep.* **2017**, *17* (6), 41.
(72) Wang, P.; You, D.; Saravia, J.; Shen, H.; Cormier, S. A. Maternal exposure to combustion generated PM inhibits pulmonary Th1 maturation and concomitantly enhances postnatal asthma development in offspring. *Part. Fibre Toxicol.* **2013**, *10* (1), 29.
(73) Wang, P.; Thevenot, P.; Saravia, J.; Ahlert, T.; Cormier, S. A. Radical-containing particles activate dendritic cells and enhance Th17 inflammation in a mouse model of asthma. *Am. J. Respir. Cell Mol. Biol.* **2011**, *45* (5), 977−983.
(74) Chauhan, A. J. Air pollution and infection in respiratory illness. *Br. Med. Bull.* **2003**, *68* (1), 95−112.
(75) Nandasena, S. Indoor air pollution and respiratory health of children in the developing world. *World J. Clin. Pediatr.* **2013**, *2* (2), 6.
(76) Sussan, T. E.; Gajghate, S.; Thimmulappa, R. K.; Ma, J.; Kim, J.-H.; Sudini, K.; Consolini, N.; Cormier, S. A.; Lomnicki, S.; Hasan, F. Exposure to electronic cigarettes impairs pulmonary anti-bacterial and anti-viral defenses in a mouse model. *PLoS One* **2015**, *10* (2), 1−15.
(77) Khachatryan, L.; Vejerano, E.; Lomnicki, S.; Dellinger, B. Environmentally persistent free radicals (EPFRs). 1. Generation of reactive oxygen species in aqueous solutions. *Environ. Sci. Technol.* **2011**, *45* (19), 8559−8566.
(78) Prahalad, A. K.; Soukup, J. M.; Inmon, J.; Willis, R.; Ghio, A. J.; Becker, S.; Gallagher, J. E. Ambient air particles: Effects on cellular oxidant radical generation in relation to particulate elemental chemistry. *Toxicol. Appl. Pharmacol.* **1999**, *158* (2), 81−91.
(79) Prahalad, A. K.; Inmon, J.; Dailey, L. A.; Madden, M. C.; Ghio, A. J.; Gallagher, J. E. Air pollution particles mediated oxidative DNA base damage in a cell free system and in human airway epithelial cells in relation to particulate metal content and bioreactivity. *Chem. Res. Toxicol.* **2001**, *14* (7), 879−887.
(80) Knaapen, A. M.; Shi, T.; Borm, P. J. A.; Schins, R. P. F. Soluble metals as well as the insoluble particle fraction are involved in cellular DNA damage induced by particulate matter. *Mol. Cell. Biochem.* **2002**, *234/235* (1), 317−326.
(81) Girotti, A. W. Mechanisms of lipid peroxidation. *J. Free Radicals Biol. Med.* **1985**, *1* (2), 87−95.
(82) Gardner, H. W. Oxygen radical chemistry of polyunsaturated fatty acids. *Free Radical Biol. Med.* **1989**, *7* (1), 65−86.
(83) Breen, A. P.; Murphy, J. A. Reactions of oxyl radicals with DNA. *Free Radical Biol. Med.* **1995**, *18* (6), 1033−1077.
(84) Cohen, D. J.; Ruthe, K. C.; Barnett, S. A. Transparent conducting $Zn_{1-x}Mg_xO$:(Al, In) thin films. *J. Appl. Phys.* **2004**, *96* (1), 459.
(85) Pryor, W. A. Oxy-radicals and related species: Their formation, lifetimes, and reactions. *Annu. Rev. Physiol.* **1986**, *48* (1), 657−667.
(86) Winterbourn, C. C. Toxicity of iron and hydrogen peroxide: The Fenton reaction. *Toxicol. Lett.* **1995**, *82*−*83*, 969−974.
(87) Kukier, U.; Ishak, C. F.; Sumner, M. E.; Miller, W. P. Composition and element solubility of magnetic and non-magnetic fly ash fractions. *Environ. Pollut.* **2003**, *123* (2), 255−266.
(88) Kohanski, M. A.; Dwyer, D. J.; Hayete, B.; Lawrence, C. A.; Collins, J. J. A common mechanism of cellular death induced by bactericidal antibiotics. *Cell* **2007**, *130* (5), 797−810.
(89) Patterson, M. C.; DiTusa, M. F.; McFerrin, C. A.; Kurtz, R. L.; Hall, R. W.; Poliakoff, E. D.; Sprunger, P. T. Formation of environmentally persistent free radicals (EPFRs) on ZnO at room temperature: Implications for the fundamental model of EPFR generation. *Chem. Phys. Lett.* **2017**, *670*, 5−10.
(90) Thibodeaux, C. A.; Poliakoff, E. D.; Kizilkaya, O.; Patterson, M. C.; DiTusa, M. F.; Kurtz, R. L.; Sprunger, P. T. Probing environmentally significant surface radicals: Crystallographic and temperature dependent adsorption of phenol on ZnO. *Chem. Phys. Lett.* **2015**, *638*, 56−60.
(91) Zhang, Z.; Yates, J. T. Band bending in semiconductors: Chemical and physical consequences at surfaces and interfaces. *Chem. Rev.* **2012**, *112* (10), 5520−5551.
(92) Schierbaum, K. D.; Weimar, U.; Göpel, W.; Kowalkowski, R. Conductance, work function and catalytic activity of SnO_2-based gas sensors. *Sens. Actuators, B* **1991**, *3* (3), 205−214.
(93) Franke, M. E.; Koplin, T. J.; Simon, U. Metal and metal oxide nanoparticles in chemiresistors: Does the nanoscale matter? *Small* **2006**, *2* (1), 36−50.
(94) Özgür, Ü.; Alivov, Y. I.; Liu, C.; Teke, A.; Reshchikov, M. A.; Doğan, S.; Avrutin, V.; Cho, S.-J.; Morkoç, H. A comprehensive review of ZnO materials and devices. *J. Appl. Phys.* **2005**, *98* (4), 041301.

DOI: 10.1021/acs.est.7b04439
Environ. Sci. Technol. 2018, 52, 2468−2481

(95) Hagfeldt, A.; Graetzel, M. Light-induced redox reactions in nanocrystalline systems. *Chem. Rev.* **1995**, *95* (1), 49−68.
(96) Albery, W. J. The transport and kinetics of photogenerated carriers in colloidal semiconductor electrode particles. *J. Electrochem. Soc.* **1984**, *131* (2), 315.
(97) Koole, R.; Groeneveld, E.; Vanmaekelbergh, D.; Meijerink, A.; de Mello Donegá, C. Size effects on semiconductor nanoparticles. In *Nanoparticles*; de Mello Donegá, C., Ed.; Springer Berlin Heidelberg: Berlin, Heidelberg, 2014; pp 13−51.
(98) Bludau, W.; Onton, A.; Heinke, W. Temperature dependence of the band gap of silicon. *J. Appl. Phys.* **1974**, *45* (4), 1846.
(99) Rabenau, T.; Simon, A.; Kremer, R. K.; Sohmen, E. The energy gaps of fullerene C_{60} and C_{70} determined from the temperature dependent microwave conductivity. *Z. Phys. B: Condens. Matter* **1993**, *90* (1), 69−72.
(100) Ouyang, M. Energy gaps in "metallic" single-walled carbon nanotubes. *Science* **2001**, *292* (5517), 702−705.
(101) Wohlers, M.; Bauer, A.; Belz, T. The mechanism of oxidation of fullerenes with molecular oxygen. *Prepr. Pap. Am. Chem. Soc. Div. Fuel Chem.* **1996**, *41* (1).
(102) Bouillard, J. X.; R'Mili, B.; Moranviller, D.; Vignes, A.; Le Bihan, O.; Ustache, A.; Bomfim, J. A. S.; Frejafon, E.; Fleury, D. Nanosafety by design: Risks from nanocomposite/nanowaste combustion. *J. Nanopart. Res.* **2013**, *15* (4), 1519.
(103) Michaelides, A.; Bocquet, M.-L.; Sautet, P.; Alavi, A.; King, D. Structures and thermodynamic phase transitions for oxygen and silver oxide phases on Ag{111}. *Chem. Phys. Lett.* **2003**, *367* (3−4), 344−350.
(104) Vella, E.; Messina, F.; Cannas, M.; Boscaino, R. Unraveling exciton dynamics in amorphous silicon dioxide: Interpretation of the optical features from 8 to 11 eV. *Phys. Rev. B: Condens. Matter Mater. Phys.* **2011**, *83* (17).10.1103/PhysRevB.83.174201
(105) Rubloff, G. W.; Lüth, H.; Grobman, W. D. Orbital energy shifts associated with chemical bonding of organic molecules on ZnO nonpolar surfaces. *Chem. Phys. Lett.* **1976**, *39* (3), 493−496.
(106) Wronski, C. R. M. The size dependence of the melting point of small particles of tin. *Br. J. Appl. Phys.* **1967**, *18* (12), 1731−1737.
(107) Couchman, P. R.; Jesser, W. A. Thermodynamic theory of size dependence of melting temperature in metals. *Nature* **1977**, *269* (5628), 481−483.
(108) Renshaw, G. D.; Roscoe, C. Thermal stability of γ-ferric oxide. *Nature* **1969**, *224* (5216), 263−264.
(109) Kido, O.; Higashino, Y.; Kamitsuji, K.; Kurumada, M.; Sato, T.; Kimura, Y.; Suzuki, H.; Saito, Y.; Kaito, C. Phase transition temperature of γ-Fe_2O_3 ultrafine particle. *J. Phys. Soc. Jpn.* **2004**, *73* (7), 2014−2016.
(110) Luttrell, T.; Halpegamage, S.; Tao, J.; Kramer, A.; Sutter, E.; Batzill, M. Why is anatase a better photocatalyst than rutile? - Model studies on epitaxial TiO_2 films. *Sci. Rep.* **2015**, *4*, 4043.
(111) Czanderna, A. W.; Rao, C. N. R.; Honig, J. M. The anatase-rutile transition. Part 1. Kinetics of the transformation of pure anatase. *Trans. Faraday Soc.* **1958**, *54* (0), 1069−1073.
(112) Satoh, N.; Nakashima, T.; Yamamoto, K. Metastability of anatase: size dependent and irreversible anatase-rutile phase transition in atomic-level precise titania. *Sci. Rep.* **2013**, 3.
(113) Lanza, R.; Bersani, M.; Conte, L.; Martucci, A.; Canu, P.; Guglielmi, M.; Mattei, G.; Bello, V.; Centazzo, M.; Rosei, R. Effect of crystalline phase and composition on the catalytic properties of PdSn bimetallic nanoparticles in the PROX reaction. *J. Phys. Chem. C* **2014**, *118* (44), 25392−25402.
(114) Scanlon, D. O.; Dunnill, C. W.; Buckeridge, J.; Shevlin, S. A.; Logsdail, A. J.; Woodley, S. M.; Catlow, C. R. A.; Powell, M. J.; Palgrave, R. G.; Parkin, I. P. Band alignment of rutile and anatase TiO_2. *Nat. Mater.* **2013**, *12* (9), 798−801.

DOI: 10.1021/acs.est.7b04439
Environ. Sci. Technol. 2018, 52, 2468−2481